Korean J. Chem. Eng., 32(8), 1515-1521 (2015)
DOI: 10.1007/s11814-014-0357-z

pISSN: 0256-1115
eISSN: 1975-7220

Modified model for estimation of agglomerate sizes of binary mixed nanoparticles in a vibro-fluidized bed

Xizhen Liang*,, Jian Wang*, Tao Zhou*,†, Hao Duan*, and Yueming Zhou**,***

*Key Laboratory of Resources Chemistry of Nonferrous Metals, Central South University, Changsha, 410083 Hunan, China
**Fundamental Science on Radioactive Geology and Exploration Technology Laboratory,
East China Institute of Technology, Nanchang, 330013 Jiangxi, China
***Engineering Research Center of Nuclear Technology Application, East China Institute of Technology,
Ministry of Education, Nanchang, 330013 Jiangxi, China
(*Received 26 July 2014 • accepted 1 December 2014*)

Abstract−A modified model is established according to the analysis of energy balance acting on an agglomerate of binary mixed nanoparticles in a vibrated fluidized bed (VFB). The sizes of agglomerates of binary mixed nanoparticles are calculated with this model. The average agglomerate size estimated by the model of energy balance decreases with increasing superficial gas velocity. The vibration frequency had a comparatively significant impact on agglomerate sizes that seemed to change regularly and decreased with higher frequency. Both of the experimental and theoretical results showed that vibration led to a smaller agglomerate size, and the average agglomerate sizes calculated by this model provided the closest fit to those determined experimentally.

Keywords: Agglomerate Size, Model, Binary Mixed Nanoparticles, Vibrated Fluidized Bed

INTRODUCTION

In many industrial processes, such as involving foods, drugs, biomaterials and the chemical industry, it is often necessary to handle a variety of nanoparticles due to their feature of larger surface area per unit mass. For example, nanoparticles are applied with such high efficiency as catalysts, and especially in the application of mixed nano-sized catalysts in the industry they can obviously reduce the dosage of the nanoparticles and largely improve the yield of reaction because of the full use of the surfactivity of catalysts [1]. However, nanoparticles tend to agglomerate because of their strong interparticle forces. As is widely known, nanoparticles can be fluidized in the form of agglomerates. However, nanoparticles easily form slugging, plugging, channeling and agglomerates in a fluidized bed, which greatly limits the fluidization technology application.

Vibro-fluidization is a technique successfully used to disperse and improve the fluidization behavior of nanoparticles and suppress the unstable bubbling in a gas-fluidized bed [2]. With special advantages in eliminating channels, breaking up large agglomerates of nanoparticles, increasing bed expansion and reducing the minimum fluidization velocity, the vibro-fluidized bed has proven to be an effective means to overcome the cohesive forces among nanoparticles by external vibration force [3-5]. Several authors [4-8] have proved that mechanical vibration is an effective method to improve fluidization quality of nanoparticles.

Agglomerate size is one of the key factors that have a remarkable influence on the fluidization behavior of nanoparticles in VFB. It is necessary to investigate the characteristics of agglomerating size and agglomerating fluidization considering the dynamic balance of constant agglomerating-splitting. Iwadate and Horio [9] developed a mathematical model based on the balance of bed expansion force caused by bubbles and agglomerate-to-agglomerate cohesive rupture force to predict an equilibrium agglomerate size in a bubbling fluidized bed of cohesive powders. Zhou and Li [10] proposed an equation in which the joint action of the drag and collision forces is balanced by the gravitational and cohesive force. Mawatari et al. [11] proposed a force balance model which considers cohesive force (van der Waals force) and separation force (gravity, vibration and shear force by a gas flow) for estimating the agglomerate size of Geldart group C powders in a vibro-fluidized bed. The calculated agglomerate size decreased with increasing the vibration strength. Xu and Zhu [5] established a model for the prediction of agglomerate size on the basis of the energy balance between the agglomerate collision energy, the energy due to cohesive forces and the energy generated by vibration.

The experimental and theoretical modeling of single SiO_2, TiO_2 and ZnO nanoparticle agglomerate sizes in a VFB was reported by Zhou et al. [8] in our group, which predicted the agglomerate sizes based on energy balance between the agglomerate collision energy, the effective energy arising from vibration wave, energy generated by laminar shear and cohesive energy. In the present work, a modified energy balance model based on the single SiO_2, TiO_2 and ZnO nanoparticle model of Zhou et al. [8] is developed to predict the agglomerate size of binary mixed nanoparticles of SiO_2/TiO_2, SiO_2/ZnO and TiO_2/ZnO under the application of a vibrating field, such as considering the effects of nanoparticle bed expansion height on fluidization, modifying the diameter and density of single nanoparticles by using the expression of the diameter and

†To whom correspondence should be addressed.
E-mail: zhoutao@csu.edu.cn, t2zhou@hotmail.com

density of mixed nanoparticles. The agglomerate sizes calculated by the modified model are compared with the experimental data. In particular, the effect of superficial gas velocity on the average agglomerate size of the same mass ratio binary mixed nanoparticles and the vibration frequency on that of the different mass ratio mixtures are highlighted.

THEORETICAL ANALYSIS

Different studies showed that nanoparticles could be fluidized in the form of agglomerates in VFB. The phenomenon of size-segregation of agglomerates has often been observed in fluidization and characterized by a dynamic process governed by the growing of the agglomerates due to cohesive forces and fracturing of the agglomerates caused by breaking forces [6,12-14], resulting in a layered structure along the bed height; that is, smaller and usually more stable agglomerates exist at the top bed, while larger and looser ones are present at the bottom bed [5,15]. To simplify the analysis to estimate the agglomerate sizes, some simplifications are necessary: (i) the agglomerates formed are assumed as non-porous spheres, same agglomerate sizes with a mean diameter of d_a, and with the same properties; (ii) wall effects and elutriation are ignored; (iii) the effect of electrostatic forces and liquid bridging forces is not considered as the air is dried by a silica gel column; and (iv) the vibration energy is mostly absorbed by the agglomerates on the surface of the fluidized bed [16].

It is also assumed that the agglomerate tends to disrupt or break up when the total energy including collision energy, the effective vibration energy and energy generated by hydrodynamics shear is greater than cohesive energy and energy generated by gravity-buoyancy. Accordingly, the following energy balance may be attained at the breaking critical point for the agglomerate.

$$E_{coll}+E_{vib,\,eff}+E_{drag}=E_{coh}+E_{gra} \tag{1}$$

1. Collision Energy E_{coll}

Based on the models of Zhou and Li [10] and Zhou et al. [8] in our group, the expression of the collision energy between two agglomerates is

$$E_{coll}=0.0417\pi\rho_a d_a^3[(1.5\overline{P_{s,\,n}}0.652[A_t(u_g-u_{mf})^{0.4}]g\varepsilon_b)^{0.5}]^2 \tag{2}$$

where $\overline{P_{s,\,n}}$ is about 0.077, ε_b is the bed voidage which calculated with $\varepsilon_b=1-m/\rho_p A_t h_0$, u_g is the superficial gas velocity, the minimum fluidization velocity (u_{mf}) of agglomerates can be estimated with the conventional correlation by Leva [17]

$$u_{mf}=\frac{9.23\times10^{-3}d_a^{1.82}(\rho_a-\rho_g)^{0.94}}{\mu_g^{0.88}\rho_g^{0.06}} \tag{3}$$

where μ_g and ρ_g are the viscosity and density of the fluidizing gas.

2. Effective Vibration Energy $E_{vib,\,eff}$

The application of an external vibration in the fluidization is required to overcome the adhesion force between nanoparticles for the improvement of fluidization behavior, which is advantageous to the breaking of agglomerates, and improves the uniformity and stability of a fluidized bed. Therefore, it is essential to take into account the efficient transfer of vibration energy.

During the vibration propagation wave in the medium, it is inevitable to produce an energy loss due to medium viscosity effect, irreversible deformation and friction damping effect. Moreover, the fluidized bed is heterogeneous, and the fluctuation characteristics of the bed are also heterogeneous, resulting in energy attenuation. Therefore, the effective vibration energy defined to account for the effective part of the oscillating energy that contributes to break the agglomerate, the same as based on Zhou et al. [8], the effective vibration energy is obtained as follows:

$$E_{vib,\,eff}=\left[2\times10^{-13}\left(\frac{d_p}{h_0}\right)+0.016\right]\cdot\frac{1}{3}\pi^2\rho_a d_a^3 f^2 A^2 \tag{4}$$

3. Energy Generated by Hydrodynamics Shear E_{drag}

At the minimum fluidization velocity, the kinetic or drag force for nanoparticles or agglomerates in a fluidized bed in creeping flow is given by [18]

$$F_{drag}=\frac{\pi}{8}[2.25+0.36(Re\varepsilon_a^{-n})^{0.37}]^{3.45}\rho_g^{-0.07}\mu_g^{1.07}(u_g d_a\varepsilon_a^{-n})^{0.93} \tag{5}$$

Energy generated by hydrodynamics shear is obtained as

$$E_{drag}=2\int_0^{Z_0+\alpha_{max}}F_{drag}d\delta \tag{6}$$

where δ is the displacement of the two parts of the agglomerates at the breakage or the distance between the two departing nanoparticles; Z_0 is the initial distance between the two adjacent nanoparticles, which is normally chosen as 4.0×10^{-10} m [5]; α_{max} is the maximum compression displacement [8]; ε_a is the mixed agglomerate voidage and will be discussed in the following part.

Substituting Eq. (5) into Eq. (6) gives

$$E_{drag}=\frac{\pi}{4}[2.25+0.36(Re\varepsilon_a^{-n})^{0.37}]^{3.45}\rho_g^{-0.07}\mu_g^{1.07}(u_g d_a\varepsilon_a^{-n})^{0.93}[\alpha_{max}+Z_0] \tag{7}$$

4. Cohesive Energy E_{coh}

During the fluidization, we can assume that the agglomerates of nanoparticles in collision breaks into two equal parts due to the action of attractive forces such as the van der Waals forces, which must overcome the tensile strength due to cohesive forces within the agglomerates, and the energy required for this process is the cohesion energy, E_{coh}. Assuming the cohesive forces remain constant during the breaking of the agglomerate, E_{coh} can be calculated as Zhou et al. [8]:

$$\begin{aligned}E_{coh}&=\int_{Z_0}^{Z}\frac{\pi}{4}d_a^2\frac{1-\varepsilon_a}{\varepsilon_a}1.61\varepsilon_a^{-1.48}\frac{H}{24d_p\delta^2}d\delta\\&=\frac{\pi}{96}d_a^2\frac{1-\varepsilon_a}{\varepsilon_a}1.61\varepsilon_a^{-1.48}\frac{H}{d_p}\left(\frac{1}{Z_0}-\frac{1}{Z}\right)\end{aligned} \tag{8}$$

where H is the Hamaker constant, Z is the displacement within which the tensile strength of the agglomerates remains in effect. ε_a is the average agglomerate voidage which can be determined indirectly from the mixed agglomerate density (ρ_a) and the mean particle density ($\rho_p=\rho_{p1}=\rho_{p2}$) of the binary mixed nanoparticles, which agglomerate density $\rho_a\approx1.15\rho_b$ according to the model of Zhou and

Table 1. Properties of nanoparticles

Nanoparticle	Color	Shape	Size [nm]	Primary density [kg m^{-3}]	Bulk density [kg m^{-3}]
SiO_2	White	Spheriform	20	2560	108
TiO_2	White	Spheriform	10	3850	263
ZnO	Primrose yellow	Claviform	20	5600	357

Li [10]; therefore, ρ_p, ρ_b and ε_a are given by

$$\frac{1}{\rho_p}=\frac{1}{\rho_{pi}}=\sum_{i=1}^{2}\frac{x_i'}{\rho_{pi}}, \quad \frac{1}{\rho_b}=\frac{1}{\rho_{bi}}=\sum_{i=1}^{2}\frac{x_i'}{\rho_{bi}}, \tag{9}$$

$$\varepsilon_a=1-\frac{\rho_a}{\rho_p} \tag{10}$$

Xu and Zhu [5] assumed that Z is to be far larger than Z_0, which is slightly larger than the lattice constant of weekly van der Waals-bonded molecular crystals [18,19]. With this hypothesis, Eq. (8) can be simplified as

$$E_{coh}=\frac{\pi}{96}d_a^2\frac{1-\varepsilon_a}{\varepsilon_a}1.61\varepsilon_a^{-1.48}\frac{H}{d_p}\frac{1}{Z_0} \tag{11}$$

where d_p is the average diameter of the mixed nanoparticles. In our study, d_{p1} and d_{p2} are the mean particle diameter of the mixed nanoparticle 1 and mixed nanoparticle 2, respectively, and $d_p=d_{p1}=d_{p2}$. The mean particle diameter of the binary mixed nanoparticles can be calculated by

$$\frac{1}{d_{pi}}=\sum_{i=1}^{2}\frac{x_i'}{d_{pi}}, \tag{12}$$

H is the Hamaker constant, which can be calculated by the following equation [20]:

$$H=\frac{3}{4}BT\left(\frac{\varepsilon_1-\varepsilon_0}{\varepsilon_1+\varepsilon_0}\right)^2+\frac{3h'v_e}{16\sqrt{2}}\frac{(N_1^2-N_0^2)^2}{(N_1^2+N_0^2)^{1.5}} \tag{13}$$

where B is Boltzmann's constant ($B=1.381\times10^{-23}$ J K^{-1}), h′ is Planck's constant ($h=6.626\times10^{-34}$ J s), T is the absolute temperature, ε_1 is the dielectric constant of mixed nanoparticles, N_1 is the index of refraction of mixed nanoparticles (for vacuum or air, $\varepsilon_0=N_0=1$), v_e is ultraviolet (UV) adsorptive frequency, typically at around 3×10^{15} s^{-1}. According to the Physical Properties Handbook, the dielectric constants of used SiO_2, TiO_2 and ZnO nanoparticles are 3.7, 40-60 and 1.6-2.6, and index of refractions are 1.5422, 2.493 and 1.9, respectively. The dielectric constant and the index of refraction of different mass ratio mixed binary nanoparticles can be calculated by the arithmetic average approximate value of different mass nanoparticles. Therefore, the corresponding Hamaker constant value can be achieved.

5. Energy Generated by Gravity-buoyancy E_{gra}

According to the model of Zhou and Li [10], for one agglomerate during stable fluidization, the difference between gravitational force and buoyancy F_{gra} is given by

$$F_{gra}=\frac{\pi}{6}(\rho_a-\rho_g)d_a^3g \tag{14}$$

Then E_{gra} is obtained as

$$E_{gra}=F_{gra}\Delta h=\frac{\pi}{6}(\rho_a-\rho_g)d_a^3g\Delta h \tag{15}$$

where Δh is bed expansion height during stable fluidization [21].

Anyhow, substituting Eqs. (2), (4), (7), (11) and (15) into Eq. (1), and determining the various parameters and substituting them into the corresponding formula, then the agglomerate size can be estimated.

EXPERIMENTAL

The schematic diagram of the vertical vibrated fluidized bed for nanoparticles is as described in our previous work [15,21]. The laboratory scale fluidization column (bed diameter 40 mm and 700 mm high) is made of Plexiglas for visually observing the bed of nanoparticles, and equipped with a porous plate gas distributor. Compressed air whose superficial gas velocity (u_g) was controlled by a rotameter in the range of 0-0.132 m s^{-1}, the vibration amplitude was set at 3.0 mm and the vibration frequency of was determined by a transducer varying from 0 to 45 Hz. The particulate materials were SiO_2, TiO_2, and ZnO nanoparticles, whose key physical properties are also listed in Table 1. Two kinds of different mass ratio primary nanoparticles were mixed uniformly and loaded onto the bed after the sieved (35-mesh sieve opening) and broken secondary agglomerates, which many nanoparticles form large and compact agglomerates simply are difficult to fluidize due to the large cohesive forces between the nanoparticles. Therefore, removing agglomerates larger than 500 μm would usually improve fluidization quality [22]. The bed height was fixed about 40 mm before the experiments started.

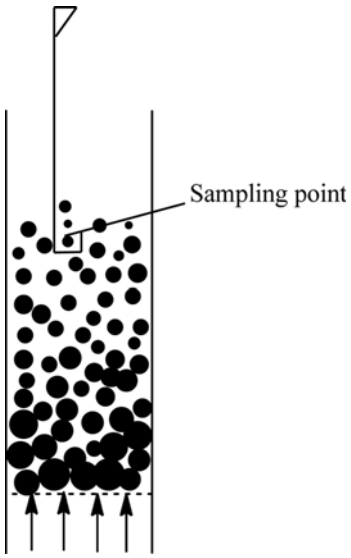

Fig. 1. Schematic diagram of the sampling positions used.

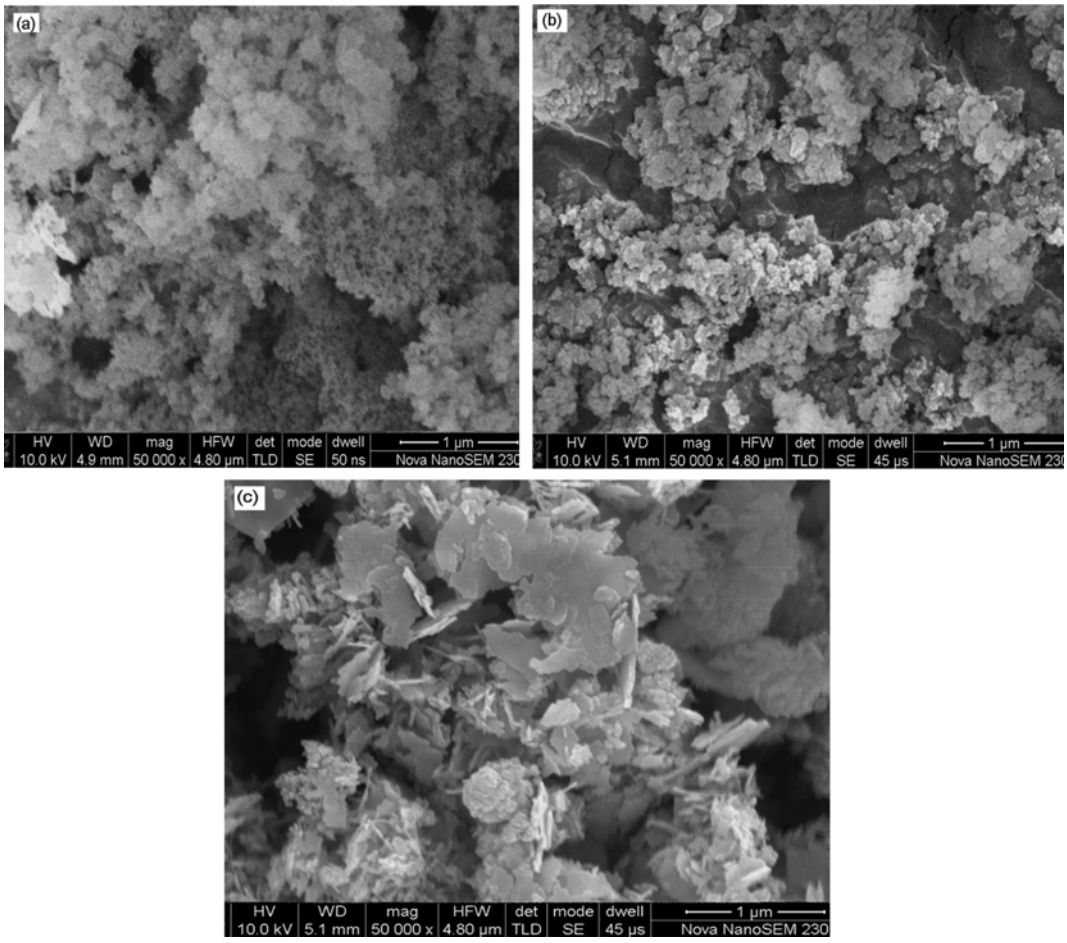

Fig. 2. SEM images of the top-bed agglomerates of the binary mixed nanoparticles with the same mass ratio.

The homogenized fluidized binary mixed agglomerates of different mass ratio nanoparticles were taken out carefully from the different axial and radial locations in the top bed while the bed was completely fluidized (after 30 min [15]) with a sampling ladle self-made to avoid disruption of their size, structure, and shape, as shown in Fig. 1. In the present work, a layered structure of agglomerates is often observed along the bed height, which has a bottom more dense layer consisting of very large agglomerates and a top less dense layer consisting of very smoothly fluidized smaller agglomerates. To avoid a large agglomerate size distribution, only the top smooth fluidization portion of the bed was used. Fig. 2 shows scanning electron microscope (SEM) pictures of typical agglomerate structures of SiO_2/TiO_2, SiO_2/ZnO and TiO_2/ZnO nanoparticle mixtures with the same mass ratio sampled from the top-bed at smooth fluidization. It can be observed from SEM images (see Fig. 2) that the agglomerates are not spherical due to the random orientation of irregular agglomerates in the gas flow, but are close to spherical in the positive position metallographic microscope--an optical microscope whose lens has a scale which is used to measure the agglomerate size (see Fig. 3). We assumed that the agglomerates could be represented as spheres using equivalent diameter defined as the average value of five measurement lengths. Therefore, the mixed agglomerate samples were directly analyzed by a positive position metallographic microscope in order to minimize distortion of the weak agglomerates. To reduce experimental error, the length across the agglomerate was measured five times at different directions. For

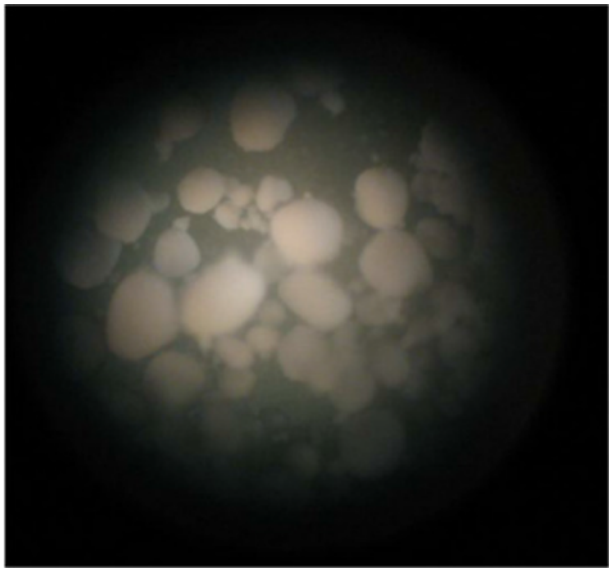

Fig. 3. Optical microscope image from the top-bed agglomerates of the binary mixed nanoparticles.

each investigation, the average agglomerate size of the nanoparticle mixture is mean value of equivalent diameters of 50 measurements. The error limit of the experimental average agglomerate diameter of different binary mixed nanoparticles under the same fluidized conditions was within the range of ± (0-15) %, giving acceptable reproducibility for this technique.

Similar to the experiments of Hakim et al. [23], the initial nanoparticle mixture agglomerates broke apart and reformed into new complex agglomerates under mechanical vibration, which offers qualitative evidence of the dynamic agglomeration of pre-existing nanoparticle agglomerates during fluidization. Fig. 2 also shows that the compositions of the nanoparticle mixture of SiO_2/TiO_2, SiO_2/ZnO and TiO_2/ZnO are variable in a wide range, but agglomerate shapes and sizes appear to be similar to each other, so it is difficult to distinguish the different composition of agglomerates [24]. There are different agglomerate sizes between different mixtures (Fig. 2(a), (b), (c)), probably due to the differences in level of interparticle forces and physical properties.

RESULTS AND DISCUSSION

1. Estimation of Agglomerate Sizes of Binary Mixed Nanoparticles with Various Superficial Gas Velocity

According to the analysis of the probability of agglomerate coalescence and breakup [25], it can be seen that the superficial gas velocity is one of the major factors affecting agglomeration sizes. At a fixed vibration condition (f=40 Hz, A=3.0 mm) and fluidization time 30 min, the influence of u_g on d_a of the same mass ratio binary mixtures of SiO_2/TiO_2, SiO_2/ZnO and TiO_2/ZnO nanoparticles is shown in Fig. 4. The results indicate that the measured average agglomerate sizes of three nanoparticle mixtures decreases with increasing superficial gas velocity; when u_g>0.084 m/s, these trends slow down, which is in agreement with those data calculated by the above model with different u_g (see Fig. 3) and consistent with the prediction results by Zhou et al. [8] and Kaliyaperumal et al. [26]. However, the formation of agglomerate sizes is the result of a dynamic equilibrium [4,12]; higher gas velocity can increase the breaking force and lead to smaller agglomerates, and also can form larger agglomerate at larger cohesive force due to the increased collision probability. Therefore, the average agglomerate sizes between calculated values and experiment data fit very well when the sampling point is set at u_g=0.123 m/s.

Moreover, as shown in Fig. 4, the agglomerate sizes of the same mass ratio binary TiO_2/ZnO nanoparticle mixtures are smaller than SiO_2/TiO_2, SiO_2/ZnO nanoparticle mixtures at the same u_g from both experiments and calculation by the above model. This may be because beds made of more dense powders hinder the propagation of the vibration in a greater extent than the less dense ones.

2. Estimation of Agglomerate Sizes of Various Mass Ratio Binary Mixed Nanoparticles with Different Vibration Frequency

Unquestionably, the vibration imposed on the fluidized bed allows control of the nanoparticle agglomerates; meanwhile, the vibration energy applied to the bed facilitates the avoidance of agglomerates due to cohesion partly but also improves the overall agglomerate formation. This controversial behavior strongly depends on the physical properties of the primary nanoparticles and the vibration conditions. However, vibration frequency has a comparatively more significant effect on agglomerate sizes than vibration amplitude due to resonance vibration [7]. Therefore, the different mass ratio binary mixed nanoparticles were carried out with fixed vibration amplitude 3.0 mm and sampled with the superficial gas velocity at 0.123 m/s when fluidization time was 30 min, and agglomerate sizes was measured with different frequency, which the calculated (abbreviated to 'cal' in Fig.) and experimental (abbreviated to 'exp' in Fig.) agglomerate sizes are presented in Figs. 5-7.

From Fig. 5, with increasing vibration frequency, there is a tendency of agglomerate size of SiO_2/TiO_2 nanoparticle mixtures decreasing whether by the experimental data or calculated values by the model. For the mixtures of different mass ratio (SiO_2 : TiO_2=

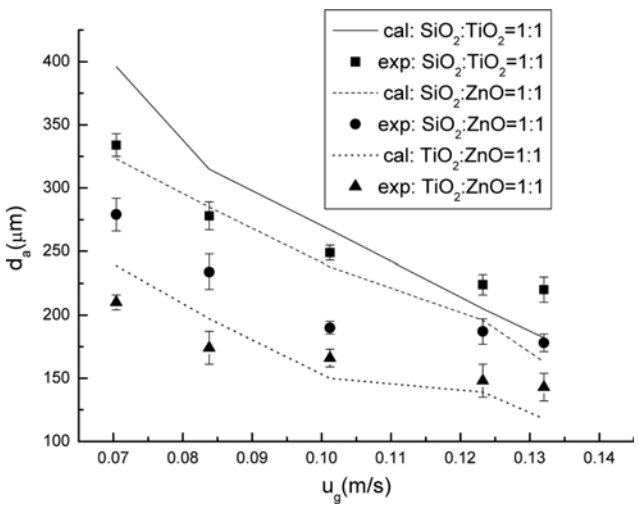

Fig. 4. Comparison of the calculated and experimental agglomerate sizes for the same mass ratio binary mixed nanoparticles with u_g.

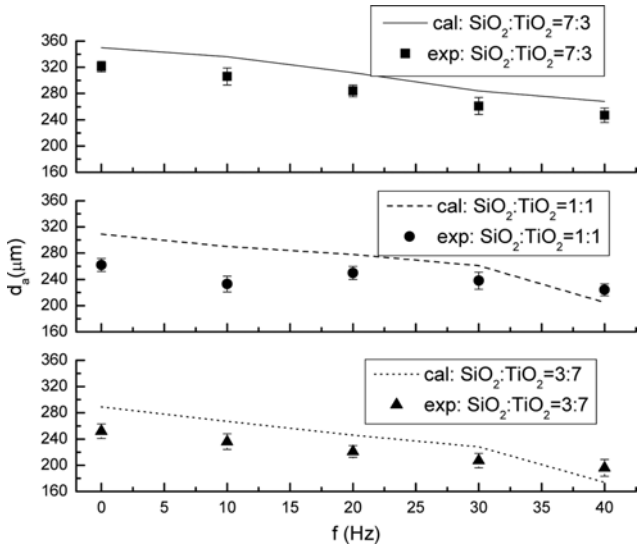

Fig. 5. Comparison of the calculated and experimental agglomerate sizes for the different mass ratio binary mixtures of SiO_2/TiO_2 nanoparticles.

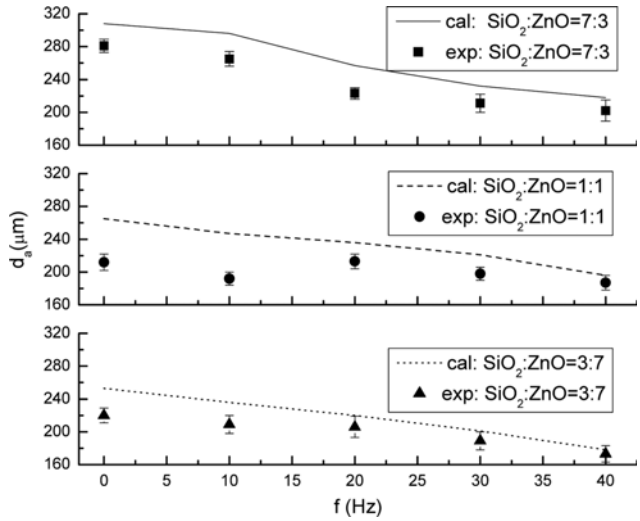

Fig. 6. Comparison of the calculated and experimental agglomerate sizes for the different mass ratio binary mixtures of SiO_2/ZnO nanoparticles.

7 : 3; 1 : 1; 3 : 7), agglomerate sizes decrease with decreasing the mass ratio of SiO_2 component under the different frequencies, but the trend has some differences, which may be that SiO_2 nanoparticle has a relatively smaller primary density and easily forms loose and fragile agglomerates. Meanwhile, the mean agglomerate size calculated values have a good fit with the experimental data under the frequencies of more than 30 Hz, because lower frequency action affects the interparticle contact and causes more experimental error. Similar trend is also observed for SiO_2/ZnO (see Fig. 6); the calculated agglomerate sizes of different mass ratio mixtures (SiO_2 : ZnO= 7 : 3; 1 : 1; 3 : 7) fit well with the experimental mean data in the range of frequency.

Compared with the two kinds of mixtures of containing SiO_2 nanoparticle, the agglomerate sizes of different mass ratio TiO_2/ZnO (see Fig. 7) obtained smaller agglomerate sizes under the same conditions. These different behaviors are due to the different nature of nanoparticles: in particular, the intrinsic higher bulk density and smaller size of TiO_2 and ZnO nanoparticles compared to the SiO_2 nanoparticles. Moreover, both experimental and theoretical studies show that a higher frequency leads to a smaller agglomerate size, although occasionally a little fluctuation. Especially to the different mass ratio (TiO_2 : ZnO=3 : 7), the agglomerate size of experimental values in turn is more than the calculated data at higher frequency(f>30 Hz), which may be due to more narrow size distribution of nanoparticles mixtures with the increasing of ZnO (the initial density is bigger than TiO_2) content [15]. At the same time, higher vibration energy is also able to promote a more efficient cracking of nanoparticle agglomerates and determines a significant reduction of agglomerate sizes [27]. Similar results were also observed in the experiments of Hakim et al. [23].

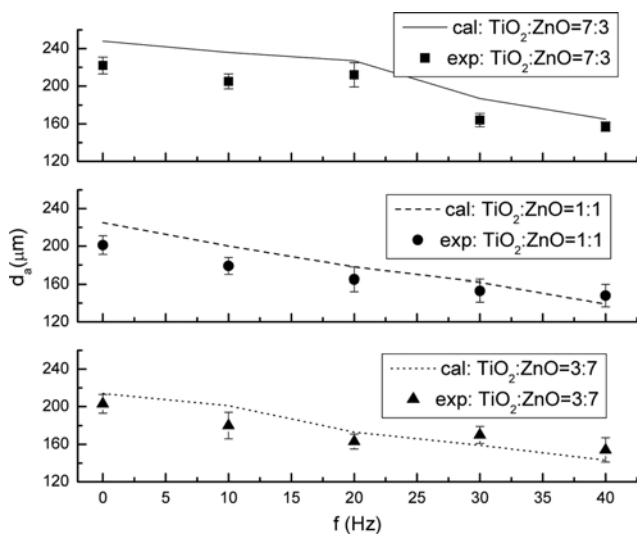

Fig. 7. Comparison of the calculated and experimental agglomerate sizes for the different mass ratio binary mixtures of TiO_2/ZnO nanoparticles.

In view of the above phenomenon, it is generally assumed that the effect of vibration frequency on the agglomeration of binary mixed nanoparticles is two-sided. First, the additional energy introduced to the bed can lead to a smaller agglomerate diameter. On the other hand, the vibration increases the contacting probability between agglomerates, which is favorable to the growth of agglomerates in fluidization of binary mixed nanoparticles. These dual effects compete with each other during the process of self-agglomeration in the fluidization state. According to the above analysis, it is concluded that the proposed model is reasonable and can predict the agglomerate sizes of three different mass ratio nanoparticle mixtures, which have the closest fit with the experimental values.

CONCLUSIONS

A modified model for the prediction of agglomerate sizes of binary mixed nanoparticles was developed on the basis of energy balance of the agglomerate collision energy, the effective vibration energy, energy generated by hydrodynamics shear, cohesive energy and energy generated by gravity-buoyancy in VFB. The results suggest that agglomerates can form, break apart, and re-agglomerate dynamically during the fluidization process. The agglomerate sizes decreased with larger superficial gas velocity, and additional vibrational energy can help to break the agglomerates, also make for the growth of the agglomerates due to the enhanced contacting probability between particles and/or agglomerates. The vibration frequency had a comparatively significant impact on agglomerate sizes, which seemed to change regularly and decreased with higher frequency. There is good agreement with the experimental data and theoretical calculated values for three different mass ratio binary mixed nanoparticles (SiO_2/TiO_2, SiO_2/ZnO, TiO_2/ZnO).

ACKNOWLEDGEMENTS

This work was financially supported by the National Natural Science Foundation of China (21176266), Open Fund of Fundamental Science on Radioactive Geology and Exploration Technology Laboratory, East China Institute of Technology (No. REGT1213) and Open Fund of Engineering Research Center of Nuclear Technology Application (East China Institute of Technology), Ministry

of Education (No. HJSJYB 2011-15). The authors are grateful to Doctor Tangwei Liu for his help offered in Matlab.

SYMBOLS USED

A : amplitude of vibration [m]
A_t : cross-section area of the fluidized bed [m^2]
d_a : the mean agglomerate diameter of binary mixture [m]
d_p : the mean particle diameter of binary mixture [m]
d_{pi} : the average particle diameter of binary mixture i [m]
d_{pi}' : the primary particle diameter of i nanoparticle in binary mixture [m]
E_{coh} : cohesive energy [J]
E_{coll} : collision energy [J]
E_{drag} : drag energy generated by hydrodynamics shear [J]
E_{gra} : energy generated by gravity-buoyancy [J]
$E_{vib,\,eff}$: effective vibration energy [J]
f : frequency of vibration [Hz]
F_{gra} : the difference between gravitational force and buoyancy [N]
g : acceleration due to gravity (=9.81) [m/s^2]
h : bed height during fluidization [m]
h_0 : initial bed height [m]
Δh : bed expansion height ($=h-h_0$) [m]
H : Hamaker constant [J]
m : the mass of the agglomerate of binary mixtures [kg]
n : exponent in the Richardson-Zaki equation [-]
$\overline{P_{s,\,n}}$: dimensionless average nanoparticle pressure [-]
Re : Reynolds number [-]
u_g : superficial gas velocity [m/s]
u_{mf} : minimum fluidization velocity [m/s]
u_t : terminal velocity for agglomerate [m/s]
x_i' : the mass fraction of nanoparticle i of binary mixture [-]
Z : the displacement between the two agglomerates [m]
Z_0 : the initial distance between two agglomerates [m]

Greek Symbols

α_{max} : the maximum compression displacement [m]
ε_a : average agglomerate voidage [-]
ε_b : average bed voidage [-]
μ_g : gas viscosity ($=1.8\times10^{-5}$) [Pa·s]
ρ_a : average density of the agglomerate [kg/m^3]
ρ_{a0} : primary average density of the agglomerate [kg/m^3]
ρ_b : average bulk density of the agglomerate [kg/m^3]
ρ_{bi} : average bulk density of binary nanoparticle mixture i [kg/m^3]
ρ_{bi}' : primary bulk density of nanoparticle i in binary mixture [kg/m^3]
ρ_g : density of air (=1.205) [kg/m^3]
ρ_p : average particle density of binary nanoparticle mixture [kg/m^3]
ρ_{pi} : average particle density of binary nanoparticle mixture i [kg/m^3]
ρ_{pi}' : the primary particle density of nanoparticle i in binary mixture [kg/m^3]
δ : distance between agglomerate or nanoparticle [m]

REFERENCES

1. M. C. Long, W. M. Cai, J. Cai, B. X. Zhou, X. Y. Chai and Y. H. Wu, *J. Phys. Chem. B*, **110**(41), 20211 (2006).
2. J. M. V. Millán, *Fluidization of fine powders*, Springer, Springer Dordrecht Heidelberg New York London (2013).
3. L. Meili, R. V. Daleffe and J. T. Freire, *Chem. Eng. Technol.*, **35**(9), 1649 (2012).
4. J. M. Valverde and A. Castellanos, *AIChE J.*, **52**(5), 1705 (2006).
5. C. B. Xu and J. Zhu, *Chem. Eng. Sci.*, **60**(23), 6529 (2005).
6. C. H. Nam, R. Pfeffer, R. N. Dave and S. Sundaresan, *AIChE J.*, **50**(8), 1776 (2004).
7. H. Wang, T. Zhou, J. S. Yang, J. J. Wang, H. Kage and Y. Mawatari, *Chem. Eng. Technol.*, **33**(3), 388 (2010).
8. L. Zhou, H. Wang, T. Zhou, K. Li, H. Kage and Y. Mawatari, *Adv. Powder Technol.*, **24**(1), 311 (2013).
9. Y. Iwadate and M. Horio, *Powder Technol.*, **100**(2), 223 (1998).
10. T. Zhou and H. Z. Li, *Powder Technol.*, **101**(1), 57 (1999).
11. Y. Mawatari, Y. Tatemoto and N. Katsuji, *J. Chem. Eng. Japan*, **36**(3), 277 (2003).
12. C. Zhu, Q. Yu, R. N. Dave and R. Pfeffer, *AIChE J.*, **51**(2), 426 (2005).
13. Y. Wang, G. S. Gu, F. Wei and J. Wu, *Powder Technol.*, **124**(1-2), 152 (2002).
14. J. S. Yang, T. Zhou and L. Y. Song, *Adv. Powder Technol.*, **20**(2), 158 (2009).
15. X. Z. Liang, H. Duan, J. Wang and T. Zhou, *Chem. Eng. Technol.*, **37**(1), 20 (2014).
16. T. J. Wang, Y. Jin, A. Tsutsumi, Z. W. Wang and Z. Cui, *Chem. Eng. J.*, **78**, 115 (2000).
17. M. Leva, *Fluidization*, McGraw-Hill, New York, 327 (1959).
18. H. Krupp, *Particle Adhesion: Theory and Experiment*, *Adv. Colloid Interface Sci.*, New York, Elsevier, **1**, 111 (1967).
19. H. Krupp and G. Sperling, *J. Appl. Phys.*, **37**(11), 4176 (1966).
20. J. N. Israelachvili, *Intermolecular and surface forces*, Academic Press, Orlando, FL (1985).
21. X. Z. Liang, H. Duan, T. Zhou and J. R. Kong, *Adv. Powder Technol.*, **25**(1), 236 (2014).
22. L. de Martín, A. Fabre and J. Ruud van Ommen, *Chem. Eng. Sci.*, **112**, 79 (2014).
23. L. F. Hakim, J. L. Portman, M. D. Casper and A. W. Weimer, *Powder Technol.*, **160**(3), 149 (2005).
24. P. Ammendola and R. Chirone, *Powder Technol.*, **201**(1), 49 (2010).
25. T. Zhou, H. Z. Li and K. Shinohara, *Adv. Powder Technol.*, **17**(2), 159 (2006).
26. S. Kaliyaperumal, S. Barghi, L. Briens, S. Rohani and J. Zhu, *Particuology*, **9**(3), 279 (2011).
27. D. Barletta and M. Poletto, *Powder Technol.*, **225**, 93 (2012).